



Article

Pomegranate Peel Derived-Carbon for Highly Efficient Palladium-Based Catalysts for Acetylene Hydrochlorination

Zonglin Li ¹, Lu Wang ^{1,2,*}, Haijun Yan ^{1,*}, Jindou Liu ¹, Shahid Ali ^{1,3}, Chao Yang ¹, Ronglan Wu ¹, Jide Wang ¹, Yana Wei ^{2,*}, Hui Sun ^{1,4} and Changhai Liang ⁵

- Key Laboratory of Oil and Gas Fine Chemicals, Ministry of Education & Xinjiang Uygur Autonomous Region, School of Chemical Engineering, Xinjiang University, Urumqi 830017, China; lizonglin124@163.com (Z.L.); 13999104116@163.com (J.L.); shahidali52035@gmail.com (S.A.); jerryyang1924@163.com (C.Y.); wuronglan@163.com (R.W.); awangid@126.com (J.W.); sunhui@ecust.edu.cn (H.S.)
- School of Petroleum and Chemical Engineering, Xinjiang Applied Vocational Technical College, Kuitun 833200, China
- Polytechnic Institute, Institute of Zhejiang University-Quzhou, Zhejiang University, Quzhou 324000, China
- State Key Laboratory of Chemical Engineering, School of Chemical Engineering, East China University of Science and Technology, Shanghai 200237, China
- State Key Laboratory of Fine Chemicals, Dalian University of Technology, Dalian 116086, China; changhai@dlut.edu.cn
- Correspondence: wanglu_4951@163.com (L.W.); yanhaijun@xju.edu.cn (H.Y.); 13999707661@163.com (Y.W.)

Abstract

A series of porous carbons (PPC) derived from pomegranate peel were synthesized as catalyst supports for Pd/PPC catalysts via hydrothermal-carbonization and incipient wetness impregnation in an acetylene hydrochlorination reaction. The optimal Pd/PPC (500) catalyst with more than 99% of acetylene conversion and vinyl chloride monomer (VCM) selectivity was obtained using an orthogonal experimental design (OED) and single-factor experiments. Based on the catalytic performance and characterization of the Pd/PPC catalyst, the deactivation mechanism of the catalysts, which was attributed to carbon deposition on the catalysts' surface, and the loss of active Pd species have been studied, which provides insights for the rational design of high-performance biomass-based acetylene hydrochlorination catalysts.

Keywords: pomegranate peel; porous carbon; Pd catalysis; acetylene hydrochlorination



Academic Editor: Jaehoon Kim

Received: 8 August 2025 Revised: 30 September 2025 Accepted: 9 October 2025 Published: 14 October 2025

Citation: Li, Z.; Wang, L.; Yan, H.; Liu, J.; Ali, S.; Yang, C.; Wu, R.; Wang, J.; Wei, Y.; Sun, H.; et al. Pomegranate Peel Derived-Carbon for Highly Efficient Palladium-Based Catalysts for Acetylene Hydrochlorination. Catalysts 2025, 15, 983. https://doi.org/10.3390/ catal15100983

Copyright: © 2025 by the authors. Licensee MDPI, Basel, Switzerland. This article is an open access article distributed under the terms and conditions of the Creative Commons Attribution (CC BY) license (https://creativecommons.org/licenses/by/4.0/).

1. Introduction

Polyvinyl chloride (PVC) is widely used in industry, agriculture, national defense, building materials and other important fields, and vinyl chloride monomer (VCM) is one of the key chemical intermediates produced by the acetylene hydrochlorination method for industrial PVC production, especially for China, which has abundant coal, scarce oil, and limited natural gas [1]. However, the widely used activated carbon (AC)-supported mercury chloride (HgCl₂) catalysts in industry face significant challenges, including mercury pollution, scarcity of mercury resources, and constraints imposed by mercury restriction policies such as the Minamata Convention [2]. Consequently, the development of highly efficient and stable mercury-free catalysts is crucial for achieving sustainable development in the PVC industry [3]. Additionally, given the presence of highly corrosive media such as hydrogen chloride and metal chlorides in the reaction environment, carrier materials must exhibit excellent corrosion resistance [4–6]. Compared with zeolites, halloysites, Al₂O₃, and similar materials, carbon-based materials have emerged as the preferred catalyst carriers

for acetylene hydrochlorination owing to their inherent advantages, including porous structures, exceptional chemical stability, and cost-effectiveness [7]. The commercial AC carrier is cheap but will consume a lot of fossil energy and add difficulties to emission reduction under the double carbon policy, so it is of great significance to prepare sustainable carbon sources for the development of efficient mercury-free catalysts with better performance.

Biomass-derived carbon materials (BCMs) with hierarchical pore structures, large specific surface areas and tunable surface functional groups sourced from abundant renewable resources (including forest residues, agricultural residues, municipal solid wastes, urban refuse, energy crops, and animal manure, etc.), have obtained extensive research interest in energy storage and catalysis [8,9]. However, the challenge of the large-scale disposal of agricultural waste has become increasingly prominent [10]. In the case of pomegranate, it has a large cultivation area and is one of the most popular fruits in China (especially XinJiang) [11]; however, generated pomegranate peel waste of superior quality (adjustable structure, inherently high carbon content, abundance of surface functional group, etc.) of the char formation can lead to environmental pollution [12]. The conversion of such pomegranate peel waste into functionalized biochar materials can reduce carbon emissions but also provide a raw material foundation for the development of high-value-added materials, aligning with the strategic needs of carbon neutrality and the circular economy [13–15]. Therefore, a surge of research of the biomass biochar from pomegranate peel has been reported in various fields, such as catalysis, adsorption, electrochemical energy storage, etc. [16,17]. Zarroug et al. [18] converted microwave-heated pomegranate peel into activated carbon via phosphoric acid activation, achieving a material with a high specific surface area and adsorption capacity for pharmaceutical applications. Li et al. [19] synthesized high-performance capacitor electrode materials through the carbonization and alkali activation of pomegranate peel. Recently, some researchers utilized biomass-derived carbon prepared from biomass sources (such as soybeans [20], walnut shells [21], wheat flour [22], etc.) for acetylene hydrochlorination reactions, although the catalytic performance was unsatisfactory. Combining with the problems of poor stability of carbon-based catalysts for acetylene hydrochlorination and our previous research [23-30], we considered whether there is a possible way to convert pomegranate peel waste into carbon materials with high-value utilization and in PVC production. Therefore, in this work, we prepared a series of pomegranate peel carbons (PPCs) from pomegranate peel waste and studied the PPC-supported Pd-based catalysts for acetylene hydrochlorination using an incipient wetness impregnation strategy. The optimal catalyst was obtained by orthogonal experimental design and single-factor experiment and its catalytic process during the reaction process was discussed, and the possible reaction mechanism was predicted as well, providing a new insight for advancing the rational design of high-performance biomass-based catalysts for acetylene hydrochlorination.

2. Results and Discussion

2.1. Characterization of PPC

SEM and EDS results of PPC (500) (Figure 1a) reveal a small amount of irregular pore structures with mainly C, O and N elements, verifying the successful preparation of nitrogen-enriched carbon material from the pomegranate peel. BET results (Figure 1b,c and Table S1) demonstrate that PPC (500) displays type-I curves and possesses a high surface area (2295 m² g⁻¹) with a large total pore volume (1.61 cm³·g⁻¹) and an average pore size of 2.8 nm, confirming its micro-mesoporous structure. The XRD pattern (Figure 1d) exhibits two broad peaks at $2\theta = 23^{\circ}$ and 44° , which are attributable to the (002) and (101) planes of graphitic carbon, respectively, suggesting partial graphitization with an amorphous structure [31]. In addition, the C1s spectrum of the PPC (500) support is shown in Figure 1e

Catalysts 2025, 15, 983 3 of 11

and the peaks at about 284.6 eV, 285.4 eV, 286.4 eV, 287.4 eV, 289.0 eV and 290.2 eV can be attributed to the sp²-C, sp³-C, C-O groups, C=O groups, COOH groups, and π - π * groups, respectively [32]. It is obvious that the PPC (500) support is the mixed structure of sp² hybridization and sp³ hybridization (Table S2), resulting in a certain amount of defect sites, which is good for enhancing electron transfer and anchoring the Pd species [33,34]. Raman spectroscopy (Figure 1f) further reveals characteristic D-band (1340 cm⁻¹) and G-band (1595 cm⁻¹) peaks, indicating the coexistence of disordered defect structures and ordered graphitic domains in the PPC (500) as well [35].

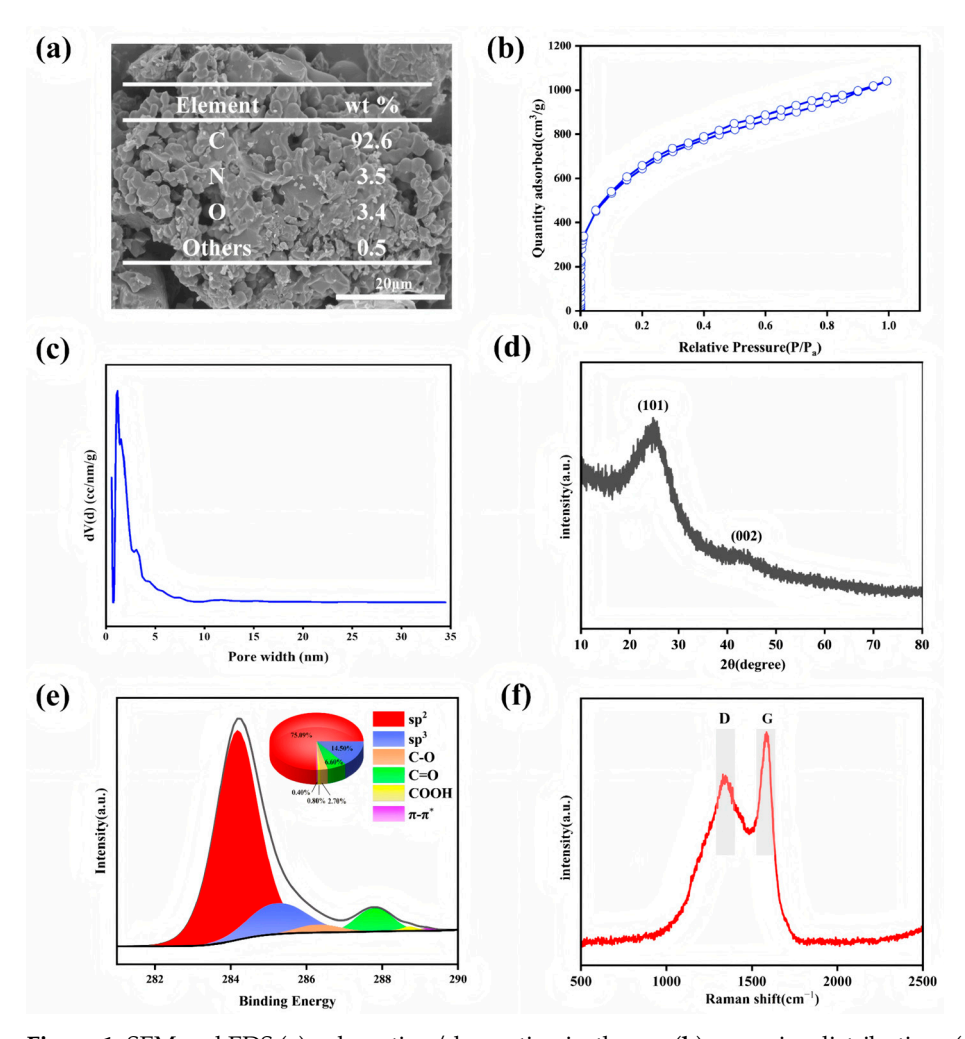


Figure 1. SEM and EDS (a), adsorption/desorption isotherms (b), pore size distributions (c) XRD (d), XPS (e) and Raman (f) results of the PPC (500).

2.2. Catalytic Performance of the Pd/PPC Catalysts

To optimize the preparation process of the Pd/PPC catalyst for acetylene hydrochlorination, an orthogonal experimental design (OED) experiment was employed to evaluate the influence of preparation conditions on catalytic performance, like hydrothermal temperature (A), hydrothermal time (B), mass ratio of $ZnCl_2$ to pomegranate peel-derived carbon (C), calcination temperature (D) and calcination time (E) (Table S3), resulting in the identification of the most critical factors for catalyst preparation [36,37]. Then, the influencing rule of the most critical factors was discussed by the single-factor experiment (Figure 2). During the OED experiment, catalyst performances of the Pd/PPC catalysts were assessed via the catalyst's activity (represented acetylene conversion) following an L^{16} (L^{5}) orthogonal array (Table S4). Based on the OED experiment design and implementation process, the results (Table S5) using the orthogonal design-direct analysis [38] revealed that

Catalysts **2025**, 15, 983 4 of 11

the sequence of influence of factors is calcination temperature (D) > mass ratio of ZnCl₂ to pomegranate peel-derived carbon (C) > hydrothermal temperature (A) > hydrothermal time (B) > calcination time (E), further confirming calcination temperature (D) as the most critical factors for the catalytic activity of the Pd/PPC catalyst for acetylene hydrochlorination. In addition, it is suggested that the optimal combination of preparation conditions may be determined as A₃B₄C₃D₂E₁, including hydrothermal temperature (180 °C), hydrothermal time (12 h), mass ratio of ZnCl₂ to pomegranate peel-derived carbon (1:1.5), calcination temperature (500 °C), and calcination time (0.5 h). To further verify the optimal calcination temperature for the Pd/PPC catalyst's preparation, the rule of the influence of calcination temperature (D) of around 500 °C was investigated by single-factor experiment (Figure 2). From Figure 2, it is suggested that the calcination temperature of Pd-based/PPC catalyst has a strong impact on the catalytic performance (stability especially) of the Pd/PPC catalyst for acetylene hydrochlorination. Compared with the PPC (Figure S1), all the Pd/PPC catalysts exhibited significantly enhanced catalytic performance after Pd loading. What is more, all the Pd/PPC catalysts showed high VCM selectivity (>95%), but their activities were decreased with the reaction time; the order of catalysts' stabilities is represented by their conversion rate as Pd/PPC (500) > Pd/PPC (700) > Pd/PPC (600) > Pd/PPC (400), and the highest acetylene conversion order is Pd/PPC (500) (99.4%) > Pd/PPC (400) (98.6%) > Pd/PPC (600) (98.2%) > Pd/PPC (700) (98.1%) (Figure 2). It is worth noting that the optimal Pd/PPC (500) catalyst achieved more than 99% of acetylene conversion and VCM selectivity during 9 h, which shows that the carbon material from the pomegranate peel can be a promising support for Pd-based catalysts in the acetylene hydrochlorination reaction.

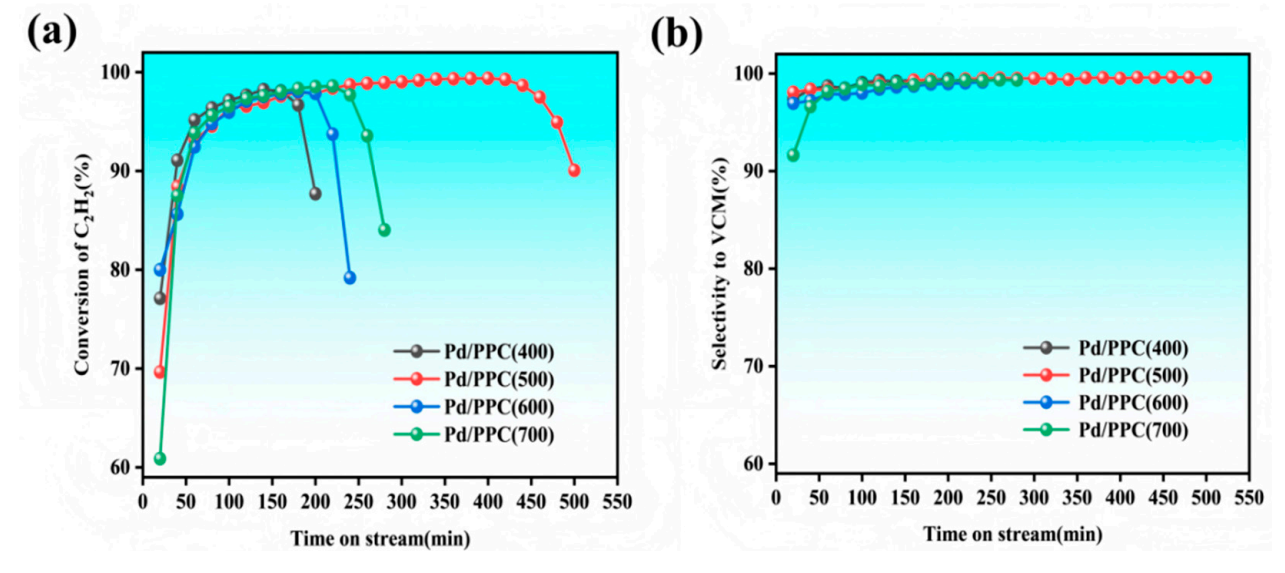


Figure 2. Acetylene conversion (a) and VCM selectivity (b) of the Pd-based/PPC catalysts.

2.3. Characterization of the Pd/PPC Catalysts

As shown in Figure 3a,d–h, elemental mapping confirms the uniform dispersion of C, N, O (sourced from pomegranate peel), and Pd species on the fresh Pd/PPC (500) catalyst. This homogeneity (consistent with EDS in Figure 1a) verifies the successful incorporation of N and Pd species. Surface morphology comparison reveals significant changes: while the fresh catalyst exhibits a smooth surface (Figure 3b), the used Pd/PPC (500) catalyst (Figure 3c) displays roughness and aggregated particles, resulting from carbon deposition and coating by reaction byproducts during acetylene hydrochlorination [39].

Catalysts **2025**, 15, 983 5 of 11

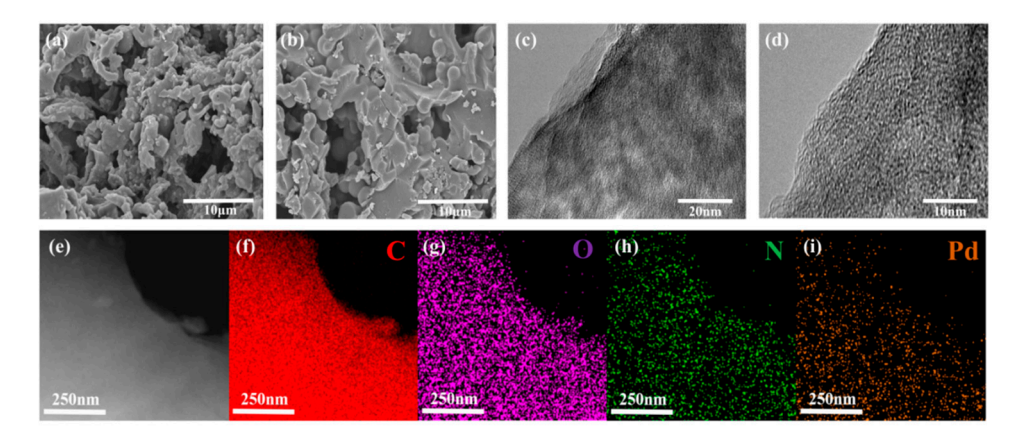


Figure 3. TEM images (**a**,**d**) and elemental mapping images (**e**-**i**) of the fresh Pd/PPC (500) catalyst; SEM images of the fresh (**b**) and used (**c**) Pd/PPC (500) catalysts.

Compared with results of the N₂ adsorption-desorption experiment of the PPC (Table S1) support and the Pd/PPC (500) catalyst (Table S6), it is suggested that the specific surface area (S_{BET}), total pore volume (V), and average pore diameter (D) of the support have changed a lot after Pd loading. The S_{BET} of the fresh Pd/PPC (500) catalyst was reduced to 2078 m²/g, the V and D also decreased to 1.50 cm³/g and 2.61 nm, respectively, resulting from the pores blocking the Pd active species. After the reaction, it is noted that the S_{BET} of the used Pd/PPC (500) decreased to 163 m²/g, but the V (0.20 cm³/g) and D (4.84 nm) increased, which indicates that micropore blockage by carbon deposits and/or Pd particle agglomeration has possibly occurred. To further prove the carbon deposition occurring on the surface of the catalyst, Thermogravimetric analysis (TGA) was performed to study the carbon deposition on the Pd/PPC (500) catalyst (Figure 4b). As can be seen in Figure 4b, the weight loss in the range of 0 °C to 100 °C can be attributed to the volatilization of the bound water in the catalyst; the weight loss in the range of 100 to 350 °C is due to the carbon deposition on the surface of the catalyst; the weight loss observed after 350 °C was caused by the combustion of the support [40]. Notably, the mass loss at the temperature ranges from 100 °C to 350 °C is due to carbon deposition on the Pd/PPC (500) catalyst surface, and the carbon content is 4.90% [41], thereby declining the catalyst's long-term stability.

To further explore the changes in the crystal structure of the Pd/PPC (500) catalyst before and after the reaction, XRD spectra of the fresh and used Pd/PPC (500) catalysts were performed in Figure 4c and two peaks at 23° and 44° belonged to the (002) and (101) crystal planes of graphite carbon, respectively, indicating that both the fresh and used Pd/PPC (500) catalysts have a certain degree of graphitization [42]. In addition, Raman results (Figure 4d) display that the I_D/I_G ratio of the used catalyst (1.79) was lower than that in the fresh catalyst (1.84), indicating that the defective domain of the used catalyst was lower than the fresh catalyst, inhibiting the dispersion of Pd species, leading to a decrease in catalyst activity of the Pd/PPC (500) catalyst [43]. Combing with XPS results (Figure 4e,f and Table S7), it is revealed that the coexistence of Pd⁰ (335.8 eV, 340.1 eV) and Pd²⁺ (337.4 eV, 342.6 eV) species is all in the Pd/PPC (500) catalysts before and after the reaction [44]. Compared with the fresh catalyst, the used Pd/PPC (500) catalyst exhibited a decreased content of Pd²⁺ species and an increased content of Pd⁰ species (Table S7), testifying that Pd²⁺ was reduced to Pd⁰ during the reaction, leading to a decline in catalytic performance of the Pd/PPC (500) catalyst consequently [45]. Furthermore, ICP results prove that the phenomenon of Pd loss is very serious and that the loss ratio of Pd species in the Pd/PPC (500) catalyst is 76.4% (Table S7), which was one of the main reasons for the deactivation of the catalyst.

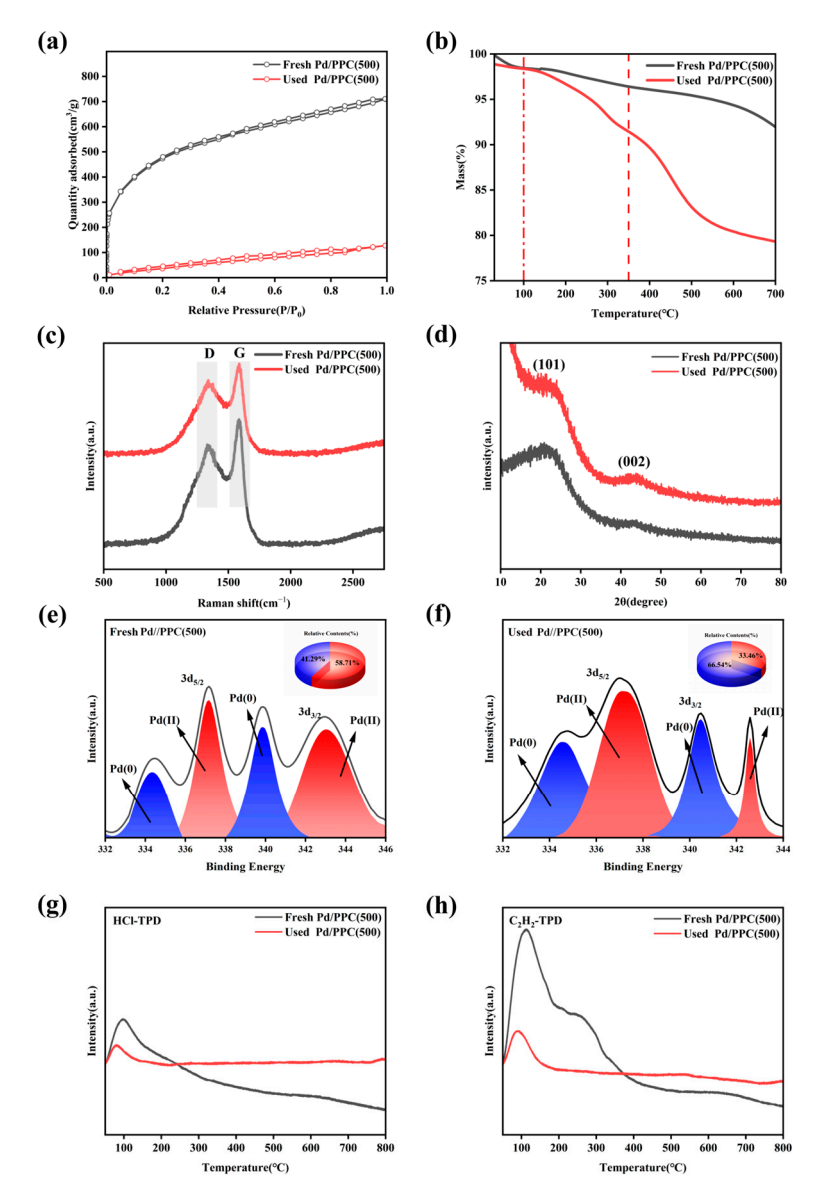


Figure 4. N₂ adsorption/desorption isotherms (**a**), TG (**b**), Raman (**c**) and XRD (**d**) characterization results of the fresh and used Pd/PPC (500) catalysts; XPS results of the fresh (**e**) and used (**f**) Pd/PPC (500) catalysts; HCl-TPD (**g**) and C_2H_2 -TPD (**h**) results of the fresh and used Pd/PPC (500) catalysts.

The adsorption properties of reactants and products on the fresh and used Pd/PPC (500) catalysts as well as the catalytic mechanism were investigated with TPD measurements (Figure 4g,h). Generally, it is suggested that the desorption temperature can indicate adsorption strength, and the peak areas can reflect adsorption capacity [46,47]. From Figure 4g, it is observed that the desorption temperature on the used the Pd/PPC (500) catalyst is lower than on the fresh one, and that the HCl desorption peak area of the used catalyst is smaller, which indicated that the HCl adsorption capacity of the used catalyst is weaker, decreasing the electron transfer from HCl to Pd^{2+} species, resulting in a decrease in the electron density around the Pd active sites. A similar rule can be observed in C_2H_2 -TPD results (Figure 4h) as well, and a stronger adsorptive capacity of the Pd/PPC (500) catalyst for C_2H_2 than for HCl in Figure 4g,h can be observed, so the possible reaction may be the following [48]: (1) the C_2H_2 molecule was adsorbed on the Pd species to form the adsorption state, followed by HCl adsorption on adjacent active centers; (2) the $C \equiv C$ bond in acetylene undergoes activation and reacts with adsorbed HCl to form vinyl chloride monomer (VCM), which is eventually desorbed from the surface of the active phase. For

the used Pd/PPC (500) catalyst, a weaker adsorption ability for HCl and C_2H_2 is obviously found, which restricts the electron transfer from the reactants (HCl and C_2H_2) to Pd²⁺ species and consequently leads to a decrease in the electron density around the Pd⁰ active sites, resulting in the catalyst deactivation.

3. Experimental Section

3.1. Catalyst Preparation

Preparation of pomegranate peel biomass-derived carbon (PPC). A total of 10 g of pomegranate peel (Yecheng County, Kashgar, Xinjiang, China) and 40 mL deionized water were mixed and hydrothermally treated at 170 °C for 12 h. Then the mixture and zinc chloride (Tianjin Zhiyuan Chemical Reagent Co., Ltd., Tianjing, China), which is beneficial for enhancing the porosity and specific surface area of PPC as a highly efficient chemical activating agent, were mixed at a mass ratio of 1:1.5 by continuous stirring for 6 h and calcined with nitrogen atmosphere at 5 °C/min to 500 °C for 0.5 h in a tubular furnace. The carbonized product was transferred to a beaker with 0.1 M HCl added and stirred for 8 h at room temperature for removing residual zinc species and other impurities. After filtration, it was also rinsed several times with deionized water until neutral, and vacuum dried at 80 °C for 12 h to achieve PPC. The series of PPC in the OED experiment were prepared by the same method with different preparation conditions, like hydrothermal temperature, hydrothermal time, ZnCl₂-pomegranate peel mass ratio, calcination temperature and calcination time. In addition, the PPC samples were calcined at 400 °C, 500 °C, 600 °C, and 700 °C denoted as PPC (400), PPC (500), PPC (600) and PPC (700), respectively.

Preparation of Pd-based catalysts supported on PPC. The Pd-based catalysts were prepared by ultrasound-assisted impregnation method, and the Pd loading capacity of all catalysts was 0.5 wt%. The general method steps are as follows: 0.033 g palladium chloride (PdCl₂) precursor was dissolved in 32.65 mL hydrogen chloride (HCl) aqueous solution. The mixture was stirred and dissolved at room temperature, which was added dropwise into 1.0 g PPC support with vigorous stirring, and an ultrasonic bath for 1 h. After impregnation at about 25 °C for 12 h and drying at 120 °C for 8 h, the Pd/PPC catalyst was obtained. The series of Pd/PPC in the OED experiment were prepared by the same method with different preparation conditions, like hydrothermal temperature, hydrothermal time, ZnCl₂-pomegranate peel mass ratio, calcination temperature and calcination time. The Pd/PPC samples were calcined at 400 °C, 500 °C, 600 °C, and 700 °C denoted as Pd/PPC (400), Pd/PPC (500), Pd/PPC (600) and Pd/PPC (700), respectively.

3.2. Catalyst Characterization

The morphology and elemental composition of the samples were evaluated using an energy-dispersive spectroscopy (EDS) device (JEOL, Tokyo, Japan) coupled with scanning electron microscopy (SEM, SU-8220, Nippon Hitachi, Tokyo, Japan). Brunauer–Emmett–Teller (BET, Quantachrome Autosorb-iQ2, Beijing Jingwei Gaobo Science and Technology Co., Ltd., Beijing, China) test was used to analyze catalysts' pore structure and surface areas with JW-BK method. X-ray diffraction (XRD, Bruker D8 ADVANCE, Nasdaq, New York, NY, USA) irradiation with Cu-K α radiation (λ = 0.15407 nm) in the 2 θ range of 10–80° was conducted. Raman spectra were gathered by laser Raman spectrometer (Horiba Scientific, LabRAM HR Evolution, Tokyo, Japan). X-ray photoelectron spectroscopy (XPS, Thermo ESCALAB250XI, Thermo Scientific, Waltham, MA, USA) was used to conduct analysis with standard C1s (284.8 eV). Transmission electron microscopy (TEM) measurements by JEM-2100F (JEOL, Tokyo, Japan) with an accelerating voltage of 200 KV were used for the analysis. Thermogravimetric analysis (TGA, TA Q600, TA Instruments, New Castle, DE, USA) was performed in an air atmosphere with a flow rate of 100 mL/min and a heating

rate of 10 $^{\circ}$ C/min. Inductively coupled plasma photoemission spectroscopy (ICP-OES, Agilent ICP-OEST30, Waltham, MA, USA) was conducted and temperature-programmed desorption (HCl-TPD/C₂H₂-TPD) tests were performed using an Auto Chem II 2920 adsorber (TA Instruments Newcastle, New Castle, DE, USA).

3.3. Catalytic Performance Test

All catalysts (4 g, 60–80 mesh) were tested on a fixed-bed microreactor (inner diameter of 10 mm) under atmospheric pressure and a reaction at 160 °C, and a gas hourly space velocity of 120 h⁻¹. Hydrogen chloride (\geq 99.99%, Jinhongshan Gas Co., Ltd., Urumqi, Xinjiang, China) and acetylene (\geq 99.99%, Jinhongshan Gas Co., Ltd.) with a volume ratio of 1.25 were implemented to effectively reduce external diffusion restrictions. In addition, acetylene conversion and vinyl chloride selectivity were analyzed by gas chromatography (GC 2010 Shimadzu, Kyoto, Japan).

4. Conclusions

In conclusion, the porous carbons (PPC) derived from pomegranate peel were synthesized by hydrothermal-carbonization method, and a series of Pd/PPC catalysts via incipient wetness impregnation were prepared and applied for acetylene hydrochlorination successfully. Through orthogonal experimental design (OED) and single-factor experiments, calcination temperature as the most critical factor for the catalytic activity of the Pd/PPC catalyst for acetylene hydrochlorination and the optimal Pd/PPC (500) catalyst achieved >99% acetylene conversion and vinyl chloride monomer (VCM) selectivity under the following reaction conditions: $160~^{\circ}$ C, GHSV = $120~h^{-1}$, and V (HCl):V (C_2H_2) = 1.25. In addition, it is suggested that the carbon deposition, the depletion of active Pd²⁺ species and weakened reactant adsorption capacity are all reasons for the catalysts' deactivation by catalysts' characterization and catalytic performance tests. The results can provide insights for the rational design of high-performance biomass-based acetylene hydrochlorination catalysts.

Supplementary Materials: The following supporting information can be downloaded at https: //www.mdpi.com/article/10.3390/catal15100983/s1, Figure S1: Catalytic performance of metal-free PPC(500), reaction conditions: $T = 160\,^{\circ}\text{C}$, GHSV (C_2H_2) = 120 h $^{-1}$, V(HCl):V(C_2H_2) = 1.25; Table S1: The specific surface area and pore structure parameters of PPC; Table S2: The percentage of different carbon species in the PPC (500); Table S3: Orthogonal experiment factors and levels table; Table S4: Orthogonal experiment results' analysis of variance; Table S6: The specific surface area and pore structure parameters of the Pd/PPC (500) catalysts; Table S7: Comparison of the valence distribution of Pd species and ICP results.

Author Contributions: Z.L.: Conceptualization, Methodology, Writing—original draft; L.W.: Supervision, Project administration, Funding acquisition; H.Y.: Resources; J.L.: Supervision; S.A.: Writing—review and editing; C.Y.: Funding acquisition; R.W.: Funding acquisition; J.W.: Project administration; Y.W.: Investigation; H.S.; Supervision; C.L.: Supervision. All authors have read and agreed to the published version of the manuscript.

Funding: Financial support was received from the National Natural Science Foundation of China (Grant Nos. 22366036, 22506167), the National College Student Innovation project (202410755054), the Tianshan Talent Research Science and Technology Innovation of Xinjiang Uygur Autonomous Region (2024TSYCCX0005, 2024TSYCTD0004), the Natural Science Foundation of Xinjiang Uygur Autonomous Region (2022D01C375), the State Key Laboratory of Fine Chemicals, Dalian University of Technology (KF2304), and the Key Research and Development Projects of Xinjiang Uygur Autonomous Region (Nos. 2024B01018, 2024B01018-1, 2024B01018-2).

Data Availability Statement: All data generated or analyzed during this study are included in this published article and its Supplementary Information files.

Conflicts of Interest: The authors declare no conflicts of interest.

References

1. Liu, Y.; Zhao, L.; Zhang, Y.; Zhang, L.; Zan, X. Progress and challenges of mercury-free Catalysis for acetylene hydrochlorination. *Catalysts* **2020**, *10*, 1218. [CrossRef]

- 2. Zhong, J.; Xu, Y.; Liu, Z. Heterogeneous non-mercury catalysts for acetylene hydrochlorination: Progress, challenges, and opportunities. *Green Chem.* 2018, 20, 2412–2427. [CrossRef]
- 3. Shang, S.; Zhao, W.; Wang, Y.; Li, X.; Zhang, J.; Han, Y.; Li, W. Highly efficient Ru@ IL/AC to substitute mercuric catalyst for acetylene hydrochlorination. *ACS Catal.* **2017**, *7*, 3510–3520. [CrossRef]
- 4. Man, B.; Zhang, H.; Zhang, C.; Li, X.; Zhu, M.; Dai, B.; Zhang, J. Effect of Ru/Cl ratio on the reaction of acetylene hydrochlorination. *New J. Chem.* **2017**, *41*, 14675–14682. [CrossRef]
- 5. Krasnyakova, T.V.; Nikitenko, D.V.; Kobets, K.D.; Krasniakova, I.O.; Gogilchin, A.S.; Bugaev, A.L.; Mitchenkoet, S.A. Stereoselectivity of acetylene hydrochlorination over supported PdCl₂/C catalysts. *Kinet. Catal.* **2023**, *64*, 294–302. [CrossRef]
- Saadi, W.; Rodríguez-Sánchez, S.; Ruiz, B.; Najar-Souissi, S.; Ouederni, A.; Fuente, E. From pomegranate peels waste to one-step
 alkaline carbonate activated carbons. Prospect as sustainable adsorbent for the renewable energy production. *J. Environ. Chem.*Eng. 2022, 10, 2213–3437. [CrossRef]
- Kaiser, S.K.; Surin, I.; Amorós-Pérez, A.; Büchele, S.; Krumeich, F.; Adam, H.C.; Román-Martínez, M.C.; Lillo-Ródenas, M.A.; Pérez-Ramírez, J. Design of carbon supports for metal-catalyzed acetylene hydrochlorination. *Nat. Commun.* 2021, 12, 4016.
 [CrossRef]
- 8. Matyjasik, W.; Matus, K.; Długosz, O.; Pulit-Prociak, J.; Banach, M. Preparation of biomass waste-derived carbon dots by the thermal degradation process. *ACS Omega* **2025**, *10*, 22529–22548. [CrossRef]
- 9. Visser, E.D.; Seroka, N.S.; Khotseng, L. Catalytic properties of biochar as support material potential for direct methanol fuel cell: A review. *ACS Omega* **2023**, *8*, 40972–40981. [CrossRef]
- Portilla-Amaguaña, A.; Barraza-Burgos, J.; Guerrero-Perez, J.; Borugadda, V.B.; Dalai, A.K. Hydrothermal carbonization of green harvesting residues (GHRs) from sugar cane: Effect of temperature and water/GHR ratio on mass and energy yield. ACS Omega 2024, 9, 26325–26335. [CrossRef]
- 11. Melgarejo-Sánchez, P.; Núñez-Gómez, D.; Martínez-Nicolás, J.J.; Hernández, F.; Legua, P.; Melgarejo, P. Pomegranate variety and pomegranate plant part, relevance from bioactive point of view: A review. *Bioresour. Bioprocess.* **2021**, *8*, 2. [CrossRef] [PubMed]
- 12. Gil, M.I.; Tomás-Barberán, F.A.; Hess-Pierce, B.; HolcroftAdel, D.M.; Kader, A.A. Antioxidant activity of pomegranate juice and its relationship with phenolic composition and processing. *J. Agric. Food Chem.* **2000**, *48*, 4581–4589. [CrossRef] [PubMed]
- 13. Al-Zoreky, N. Antimicrobial activity of pomegranate (*Punica granatum* L.) fruit peels. *Int. J. Food Microbiol.* **2009**, *134*, 244–248. [CrossRef]
- 14. Aqil, F.; Munagala, R.; Vadhanam, M.V.; Kausar, H.; Jeyabalan, J.; Schultz, D.J.; Gupta, R.C. Anti-proliferative activity and protection against oxidative DNA damage by punicalagin isolated from pomegranate husk. *Food Res. Int.* **2012**, *49*, 345–353. [CrossRef]
- 15. Hosseini, A.; Razavi, B.M.; Hosseinzadeh, H. Protective effects of pomegranate (*Punica granatum*) and its main components against natural and chemical toxic agents: A comprehensive review. *Phytomedicine* **2023**, *109*, 154581. [CrossRef]
- 16. Chen, C.; Han, B.; Zhu, X.; Jiang, C.; Wang, Y. A novel pomegranate peel-derived biochar for highly efficient removal of sulfamethoxazole by activation of peroxymonosulfate through a non-radical pathway. *J. Environ. Chem. Eng.* **2022**, *10*, 108184. [CrossRef]
- 17. Khairy, G.M.; Hesham, A.M.; Jahin, E.S.; El-Korashy, S.A.; Awad, Y.M. Green synthesis of a novel eco-friendly hydro char from pomegranate peels loaded with iron nanoparticles for the removal of copper ions and methylene blue from aqueous solutions. *J. Mol. Liq.* 2022, 368, 120722. [CrossRef]
- 18. Zarroug, M.; Najar, S.; Souissi, J.A.; Menéndez, E.G.; Calvo, A. Ouederni. Fast production of activated carbon from pomegranate peels by combining microwave heating and phosphoric acid activation for paracetamol adsorption. *Environ. Eng. Sci.* **2022**, 39, 441–452. [CrossRef]
- 19. Chavan, M.S.; Suryawanshi, S.; Kumbhar, A. bio-waste originated, heterogeneous catalysts based on pomegranate peel for knoevenagel condensation: A green approach. *React. Kinet. Mech. Catal.* **2023**, *136*, 2167–2180. [CrossRef]
- 20. Shen, Z.; Liu, Y.; Han, Y.; Liu, Y.; Cao, S. Nitrogen-doped porous carbon from biomass with superior catalytic performance for acetylene hydrochlorination. *RSC Adv.* **2020**, *10*, 14556–14569. [CrossRef] [PubMed]
- 21. Wu, S.; Jiang, A.; Zhou, X.; Guo, Z.; Wang, K. Environmentally friendly high-efficient metal-free catalyst for acetylene hydrochlorination derived from walnut shell-based N-doped biochar. *Mol. Catal.* **2022**, *532*, 112719. [CrossRef]

22. Lan, G.; Wang, Y.; Qiu, Y.; Wang, X.; Liang, J.; Han, W.; Tang, H.; Liu, H.; Liu, J.; Li, Y. Wheat flour-derived N-doped mesoporous carbon extrudate as superior metal-free catalysts for acetylene hydrochlorination. *Chem. Commun.* 2018, 54, 623–626. [CrossRef] [PubMed]

- 23. Hu, D.; Wang, F.; Wang, J. Bi/AC modified with phosphoric acid as catalyst in the hydrochlorination of acetylene. *RSC Adv.* **2017**, 7,7567–7575. [CrossRef]
- 24. Wang, L.; Wang, F.; Wang, J. Enhanced stability of hydrochlorination of acetylene using polyaniline-modified Pd/HY catalysts. *Catal. Commun.* **2016**, *74*, 55–59. [CrossRef]
- 25. Wang, L.; Wang, F.; Wang, J. Non-mercury catalytic acetylene hydrochlorination over a NH₄F-urea-modified Pd/HY catalyst for vinyl chloride monomer production. *New J. Chem.* **2016**, *40*, 3019–3023. [CrossRef]
- Zhang, M.; Wang, L.; Yan, H.; Lian, L.; Si, J.; Long, Z.; Cui, X.; Wang, J.; Zhao, L.; Yang, C.; et al. Palladium-halloysite nanocomposites as an efficient heterogeneous catalyst for acetylene hydrochlorination. *J. Mater. Res. Technol.* 2021, 13, 2055–2065.
 [CrossRef]
- 27. Ali, S.; Wang, L.; Yan, H.; Yang, C.; Wang, J.; Sun, H.; Li, X.; Wu, R.; Liang, C. Enhanced catalytic performance of palladium-based catalysts modified with the dibenzofuran ligand for acetylene hydrochlorination. *Appl. Organomet. Chem.* **2024**, *38*, 119382–119391. [CrossRef]
- 28. Lian, L.; Wang, L.; Yan, H.; Lian, L.; Wang, L.; Yan, H.; Ali, S.; Wang, J.; Zhao, L.; Yang, C.; et al. Non-mercury catalytic acetylene hydrochlorination over Bi/CNTs catalysts for vinyl chloride monomer production. *J. Mater. Res. Technol-JMRT.* **2020**, 9, 14961–14968. [CrossRef]
- Dang, L.; Wang, L.; Yan, H.; Long, Z.; Yang, C.; Wang, J.; Guan, Q.; Sun, H.; Li, X.; Wu, R.; et al. Metal immobilized in a USY zeolite-supported (4-CB) TPPB: A new strategy of enhanced stability for acetylene hydrochlorination. *Microporous Mesoporous Mat.* 2024, 377, 113204. [CrossRef]
- 30. Yang, H.; Wang, L.; Yan, H.; Dang, L.; Wang, J.; Sun, H. Hierarchical porous carbon from PVC plastic wastes with efficient catalytic performance for acetylene hydrochlorination. *New J. Chem.* **2025**, *49*, 36125–36142. [CrossRef]
- 31. Fan, Y.; Xu, H.; Gao, G.; Wang, M.; Huang, W.; Ma, L.; Yao, Y.; Qu, Z.; Xie, P.; Dai, B.; et al. Asymmetric Ru-In atomic pairs promote highly active and stable acetylene hydrochlorination. *Nat. Commun.* **2024**, *15*, 6035. [CrossRef]
- 32. Yang, Y.; Zhao, C.; Qiao, X.; Guan, Q.; Li, W. Regulating the coordination environment of Ru single-atom catalysts and unravelling the reaction path of acetylene hydrochlorination. *Green Energy Environ.* **2023**, *8*, 1141–1153. [CrossRef]
- 33. Yang, L.Q.; Zhang, C.; Li, W.L.; Li, W.; Liu, G.; Wu, M.; Liu, J.; Zhang, J. Global optimization of process parameters for low-temperature SiN_x based on orthogonal experiments. *Adv. Manuf.* **2023**, *11*, 181–190. [CrossRef]
- 34. Liu, D.; Xia, S.; Tang, H.; Zhong, D.; Wang, B.; Cai, X.; Lin, R. Parameter optimization of PEMFC stack under steady working condition using orthogonal experimental design. *Int. J. Energy Res.* **2019**, *43*, 2571–2582. [CrossRef]
- 35. Zhou, L. Preparation of calcium fluoride using phosphogypsum by orthogonal experiment. *Open Chem.* **2018**, *16*, 864–868. [CrossRef]
- 36. Qiu, Y.; Ali, S.; Lan, G.; Tong, H.; Fan, J.; Liu, H.; Li, B.; Han, W.; Tang, H.; Liu, H.; et al. Defect-rich activated carbons as active and stable metal-free catalyst for acetylene hydrochlorination. *Carbon* **2019**, *146*, 406–412. [CrossRef]
- 37. Ma, X.; Bai, Y.; Chen, S.; He, Z.; Wu, P.; Qi, Y.; Zhang, S. A composite of pineapple leaf-derived porous carbon integrated with ZnCo-MOF for high-performance supercapacitors. *Phys. Chem. Chem. Phys.* **2024**, *26*, 28746–28756. [CrossRef] [PubMed]
- 38. Wang, X.; Fan, D.; Lan, G.; Cheng, Z.; Sun, X.; Qiu, Y.; Han, W.; Tang, H.; Liu, H.; Zhu, Y.; et al. The reaction mechanism of acetylene hydrochlorination on defective carbon supported ruthenium catalysts identified by DFT calculations and experimental approaches. *Inorg. Chem. Front.* **2022**, *9*, 458–467. [CrossRef]
- 39. Dai, Z.B. Effect of carbon defects on the nitrogen-doped carbon catalytic performance for acetylene hydrochlorination. *Appl. Catal. A-Gen.* **2018**, *564*, 72–78.
- 40. Lu, F.; Wei, C.; Yin, X.; Zhang, L.; Zan, X. The effect of sp² content in carbon on its catalytic activity for acetylene hydrochlorination. *Nanomaterials* **2022**, *12*, 2619. [CrossRef]
- 41. Zhao, J.; Hu, K.; Yuan, X. Study on quantitative structure of coke deposition in UDH catalyst for acetylene hydrochlorination. *Energy Source Part A* **2023**, 45, 5458–5464. [CrossRef]
- 42. Lu, F.; Wang, Q.; Zhu, M.; Dai, B. Deactivation and regeneration of nitrogen doped carbon catalyst for acetylene hydrochlorination. *Molecules* **2023**, *28*, 956. [CrossRef]
- 43. Cen, Y.; Yue, Y.; Wang, S.; Lu, J.; Wang, B.; Jin, C.; Guo, L.; Hu, Z.; Zhao, J. Adsorption behavior and electron structure engineering of Pd-Based catalysts for acetylene hydrochlorination. *Catalysts* **2019**, *10*, 24–40. [CrossRef]
- 44. Wang, H.; Tian, Y.; Xu, M.; Cheng, X.; Huang, J.; Li, H.; Li, Y.; Shi, Y.; Ye, L.; Liu, H.; et al. Development of ionic liquids promoted low content ruthenium catalysts for acetylene hydrochlorination. *Catal. Today* **2024**, 434, 114696. [CrossRef]
- 45. Liu, Y.; Zhang, H.; Dong, Y.; Li, W.; Zhao, S.; Zhang, J. Characteristics of activated carbons modulate the catalytic performance for acetylene hydrochlorination. *Mol. Catal.* **2020**, *483*, 110707. [CrossRef]

Catalysts 2025, 15, 983 11 of 11

46. Liu, X.; Conte, M.; Elias, D.; Lu, L.; Morgan, D.J.; Freakley, S.J.; Johnston, P.; Kiely, C.J.; Hutchings, G.J. Investigation of the active species in the carbon-supported gold catalyst for acetylene hydrochlorination. *Catal. Sci. Technol.* **2016**, *6*, 5144–5153. [CrossRef]

- 47. Dong, X.; Liu, G.; Chen, Z.; Zhang, Q.; Xu, Y.; Liu, Z. Enhanced performance of Pd-[DBU][Cl]/AC mercury-free catalysts in acetylene hydrochlorination. *Chin. J. Catal.* 2023, 46, 137–147. [CrossRef]
- 48. Zhao, J.; Yu, Y.; Xu, X.; Di, S.; Wang, B.; Xu, H.; Ni, J.; Guo, L.; Pan, Z.; Li, X. Stabilizing Au (III) in supported-ionic-liquid-phase (SILP) catalyst using CuCl₂ via a redox mechanism. *Appl. Catal. B Environ.* **2017**, *206*, 175–183. [CrossRef]

Disclaimer/Publisher's Note: The statements, opinions and data contained in all publications are solely those of the individual author(s) and contributor(s) and not of MDPI and/or the editor(s). MDPI and/or the editor(s) disclaim responsibility for any injury to people or property resulting from any ideas, methods, instructions or products referred to in the content.